

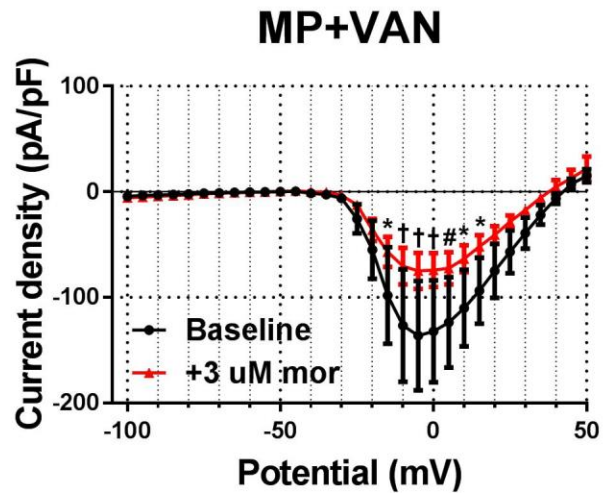
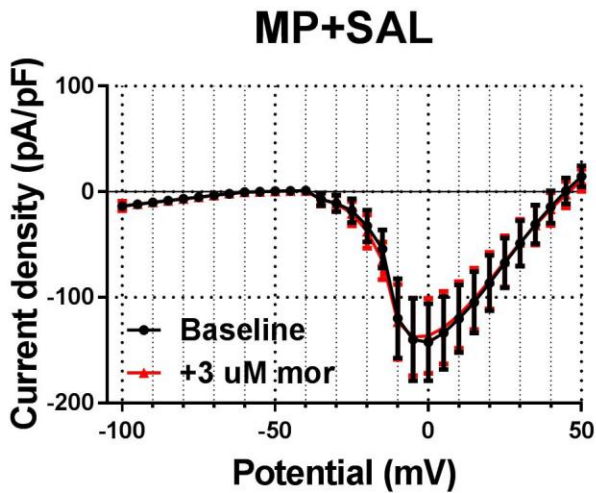
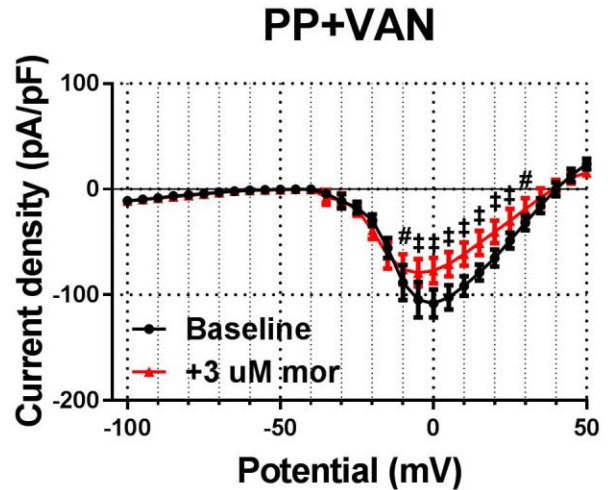
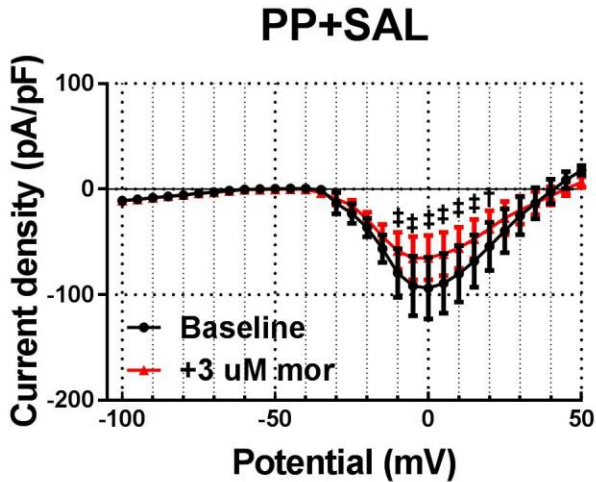
**ISCI, Volume 2**

**Supplemental Information**

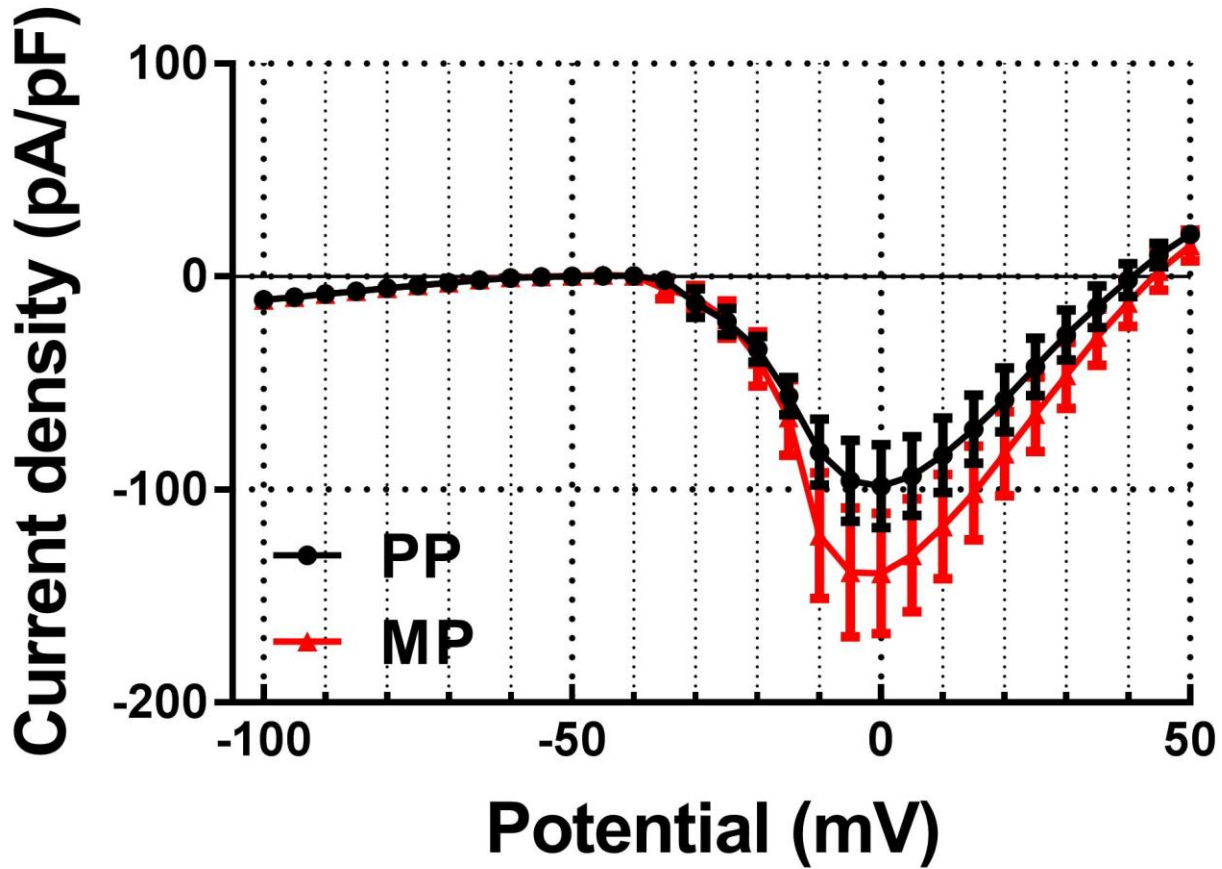
**Tolerance to Morphine-Induced Inhibition of TTX-R  
Sodium Channels in Dorsal Root Ganglia Neurons  
Is Modulated by Gut-Derived Mediators**

**Ryan A. Mischel, William L. Dewey, and Hamid I. Akbarali**

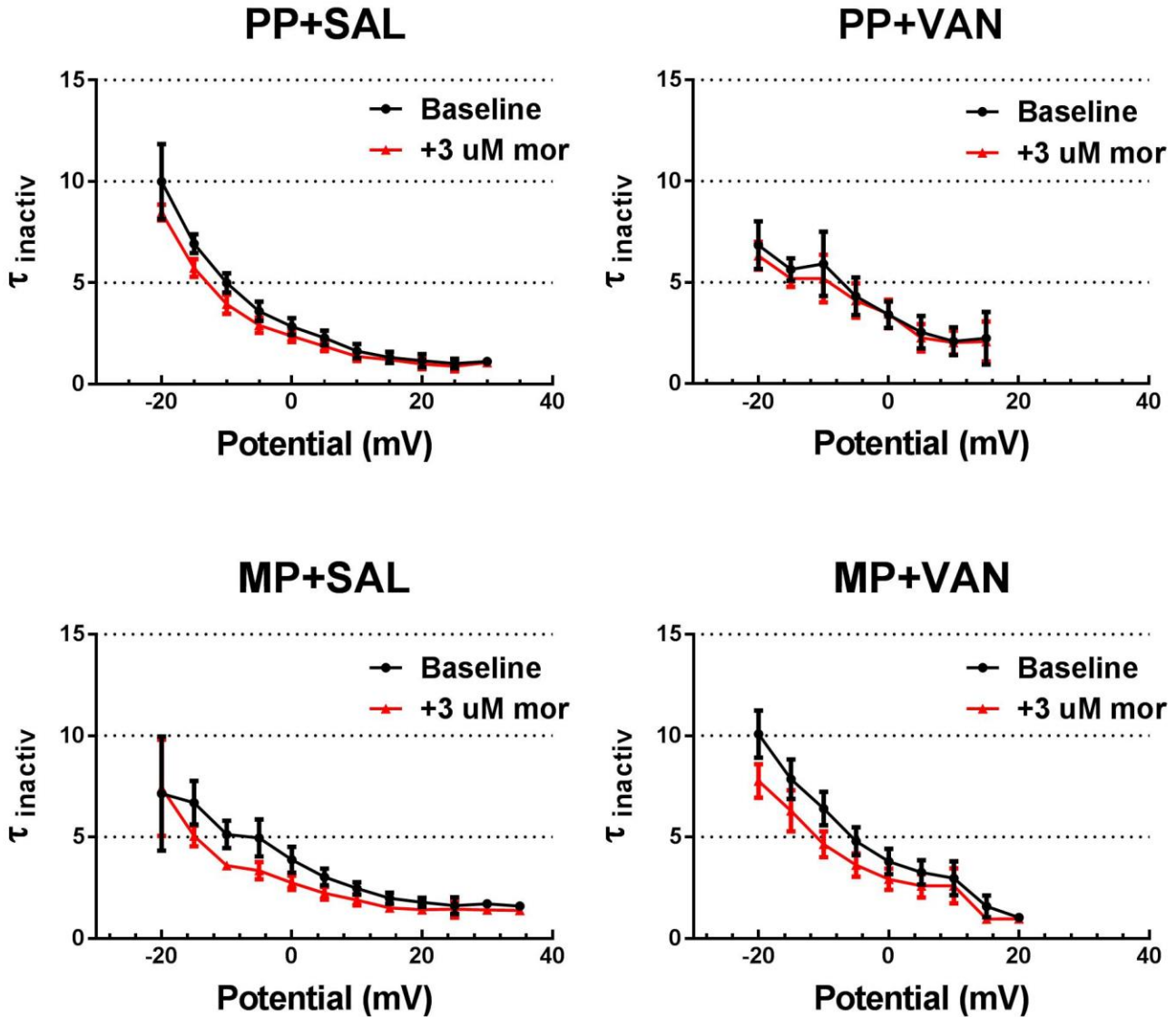
**Supplemental Figure 1: Non-normalized TTX-R Na<sup>+</sup> channel I-V curves (related to Figure 3).** Current-voltage (*I-V*) relationships of TTX-R Na<sup>+</sup> channels in voltage-clamped DRG neurons are shown at baseline (*black*) and following acute morphine challenge (3  $\mu$ M, *red*). The relatively large error bars reflect typical variance in current densities among cells. Statistical analysis reiterates the concepts presented in the text. Neurons from PP+SAL and PP+VAN mice demonstrate a significant reduction of current density for steps from -10 to +20 mV. This effect was mitigated in neurons from MP+SAL mice (indicating tolerance development), but preserved in neurons from MP+VAN mice (indicating tolerance prevention). PP+SAL (N=7,n=7), PP+VAN (N=4,n=6), MP+SAL (N=7,n=9), MP+VAN (N=5,n=7), \*p<0.05, #p<0.01, †p<0.001, ‡p<0.0001 by two-way repeated-measures ANOVA with Bonferroni post-hoc analysis; data expressed as mean  $\pm$  SEM.



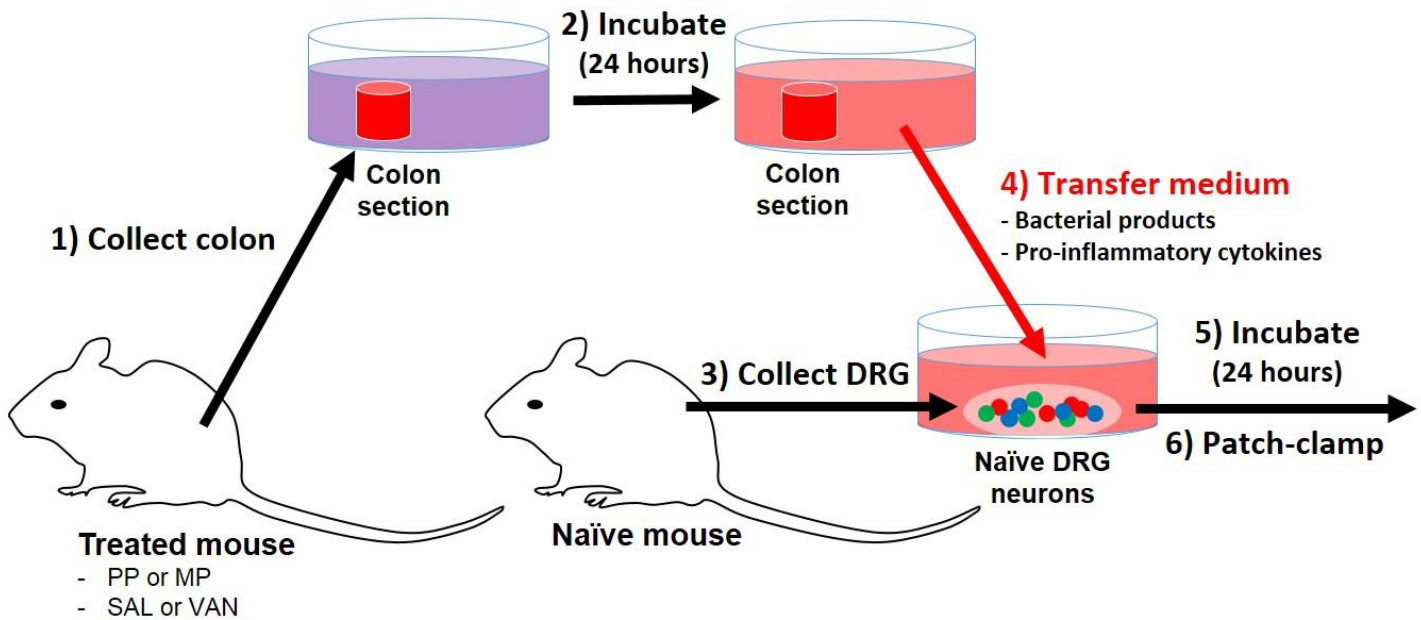
**Supplemental Figure 2: TTX-R Na<sup>+</sup> current densities trend toward enhancement in mice with chronic morphine exposure (related to Figure 4).** Non-normalized current-voltage (*I-V*) relationships of TTX-R Na<sup>+</sup> channels are shown at baseline (*black*) and following acute morphine challenge (3  $\mu$ M, *red*). Current densities demonstrate a trend toward enhancement in mice chronic morphine exposure (MP) compared to placebo (PP). However, this effect was not statistically significant in this study. PP+SAL (N=7,n=7), PP+VAN (N=4,n=6), MP+SAL (N=7,n=9), MP+VAN (N=5,n=7), analyzed by two-way repeated-measures ANOVA with Bonferroni post-hoc analysis; data expressed as mean  $\pm$  SEM.



**Supplemental Figure 3: The time constant of TTX-R Na<sup>+</sup> channel inactivation is not affected by acute morphine challenge (related to Figure 6).** Inactivation time constants ( $\tau_{inactiv}$ ) of TTX-R Na<sup>+</sup> channels at baseline (*black*) and following acute morphine challenge (3  $\mu$ M, *red*). Values were estimated by fitting a monoexponential function to the falling phase of the current traces at various step potentials. While a general trend toward reduction of  $\tau_{inactiv}$  with acute morphine challenge (3  $\mu$ M) is noted, no significant modulation was detected in any cohort. PP+SAL (N=7,n=7), PP+VAN (N=4,n=6), MP+SAL (N=7,n=9), MP+VAN (N=5,n=7), analyzed by two-way repeated-measures ANOVA with Bonferroni post-hoc analysis; data expressed as mean  $\pm$  SEM.



**Supplemental Figure 4: Schematic of sample preparation for colonic supernatant study (related to Figure 7-9).** (1) Full circumference colon segments 5 mm in length are resected from each treatment group. (2) Segments are incubated (37°C) for 24 hours in 200  $\mu$ L of supplemented neurobasal A medium, allowing mediators in the colon wall (e.g., bacterial products and pro-inflammatory cytokines) to leach out into solution. (3) L<sub>5</sub>-S<sub>1</sub> dorsal root ganglia (DRG) neurons are collected from treatment-naïve mice. (4) Colonic supernatants are transferred to naïve DRG neuron cultures along with 200  $\mu$ L of fresh medium. (5) Cultures with supernatants are incubated (37°C) for 24 hours. (6) Patch-clamp experiments are performed.



**Supplemental Table 1: Tail-flick latencies for each cohort in the vancomycin treatment duration study (related to Figure 1).**

	<b>10 day SAL</b>	<b>5 day VAN</b>	<b>10 day VAN</b>	<b>15 day VAN</b>
<b>Pre-implantation</b>	2.95±0.19	2.43±0.19	3.45±0.25	2.52±0.20
<b>Day 1</b>	10.00	10.00	9.80±0.20	10.00
<b>Day 2</b>	5.19±0.77	7.50±0.65 <sup>***</sup>	7.28±0.47 <sup>***</sup>	9.67±0.23 <sup>****, †</sup>
<b>Day 3</b>	3.26±0.20	4.38±0.34	5.98±0.43 <sup>****</sup>	9.77±0.23 <sup>****, †</sup>
<b>Day 4</b>	2.76±0.21	3.11±0.27	5.31±0.50 <sup>****</sup>	8.40±0.34 <sup>****, †</sup>
<b>Day 5</b>	2.65±0.12	2.74±0.11	5.63±0.28 <sup>****</sup>	7.60±0.29 <sup>****, †</sup>
<b>+10 mg/kg mor</b>	2.75±0.16	2.56±0.12	7.20±0.58 <sup>****</sup>	9.47±0.22 <sup>****, †</sup>

**Supplemental Table 2: Active and passive cell properties for current-clamp experiments (related to Figure 2).**

	<b>MP+VAN</b>	<b>Naloxone</b>	<b>0 mM Ca<sup>2+</sup></b>
<b>C<sub>Mem</sub> (pF)</b>	15.9±0.9	17.7±2.2	14.0±2.2
<b>R<sub>Series</sub> (MΩ)</b>	8.9±0.3	6.0±0.6	5.8±0.8
<b>V<sub>Rest</sub> (mV)</b>	-52.1±1.1	-52.9±1.8	-45.6±2.2
+3 μM morphine	-51.2±1.1	-51.9±1.7	-47.4±2.4
<b>AP (2x rheobase)</b>	1.7±0.2	1.8±0.3	--
+3 μM morphine	1.1±0.1**	1.8±0.3	--
<b>Rheobase (nA)</b>	0.31±0.03	1.11±0.14	0.15±0.05
+3 μM morphine	0.34±0.03	1.12±0.16	0.17±0.07
<b>AP V<sub>Thresh</sub> (mV)</b>	-14.5±1.2	-12.9±1.5	-12.3±2.9
+3 μM morphine	-11.3±1.4***	-12.2±1.6	-8.8±3.2*
<b>AP V<sub>Peak</sub> (mV)</b>	55.3±1.5	50.3±3.9	--
+3 μM morphine	61.9±2.2	52.8±4.3	--
<b>R<sub>input</sub> (MΩ)</b>	529.6±93.4	445.7±94.1	--
+3 μM morphine	569.8±104.5	547.3±128.5	--

**Supplemental Table 3: Descriptive values for TTX-R voltage-dependent activation studies (related to Figure 5).**

	<b>PP+SAL</b>	<b>PP+VAN</b>	<b>MP+SAL</b>	<b>MP+VAN</b>
<b>C<sub>mem</sub> (pF)</b>	12.2±1.6	14.9±1.6	14.8±1.6	15.3±2.4
<b>R<sub>series</sub> (MΩ)</b>	6.1±1.2	5.7±0.9	6.1±0.5	4.7±0.5
<b>V<sub>1/2</sub> (mV)</b>	-13.7±1.0	-16.8±1.6	-11.7±0.5	-14.1±0.3
+3 μM morphine	-15.6±1.0	-21.0±1.3	-13.0±0.5	-13.6±0.3
<b>Slope constant (k)</b>	8.10±0.91	11.05±1.42	6.24±0.48	5.32±0.28
+3 μM morphine	8.04±0.86	9.46±1.19	6.20±0.45	6.10±0.24
<b>Regression analysis</b>				
<b>p-value</b>	ns	ns	ns	ns
<b>R<sup>2</sup></b>	0.916	0.877	0.950	0.993
+3 μM morphine	0.923	0.889	0.955	0.996
<b>F</b>	0.7	1.7	1.0	1.8
<b>ΔAIC</b>	-5.5	-1.4	-4.4	-1.5



**Supplemental Table 4: Descriptive values for TTX-R steady-state inactivation studies (related to Figure 6).**

	<b>PP+SAL</b>	<b>PP+VAN</b>	<b>MP+SAL</b>	<b>MP+VAN</b>
<b>C<sub>mem</sub> (pF)</b>	12.2±1.6	14.9±1.6	14.8±1.6	15.3±2.4
<b>R<sub>series</sub> (MΩ)</b>	6.1±1.2	5.7±0.9	6.1±0.5	4.7±0.5
<b>V<sub>1/2</sub> (mV)</b>	-30.8±1.6	-34.9±2.1	-22.3±2.3	-29.2±1.1
+3 μM morphine	-31.4±2.8	-37.0±3.9	-24.3±2.3	-34.2±1.6
<b>(I/I<sub>max</sub>)<sub>max</sub></b>	1.01±0.02	0.99±0.03	0.98±0.02	1.01±0.01
+3 μM morphine	0.67±0.02	0.57±0.03	0.95±0.02	0.66±0.01
<b>(I/I<sub>max</sub>)<sub>min</sub></b>	0.32±0.01	0.20±0.02	0.34±0.02	0.23±0.01
+3 μM morphine	0.20±0.02	0.08±0.02	0.31±0.02	0.13±0.01
<b>Slope constant (k)</b>	14.06±1.52	12.11±1.98	12.38±1.18	15.18±1.06
+3 μM morphine	11.37±2.54	10.91±1.44	11.42±1.11	13.03±1.45
<b>Regression analysis</b>				
<b>p-value</b>	<0.0001	<0.0001	ns	<0.0001
<b>R<sup>2</sup></b>	0.905	0.847	0.747	0.959
+3 μM morphine	0.699	0.581	0.717	0.901
<b>F</b>	104.9	64.0	2.1	310.3
<b>ΔAIC</b>	277.0	181.9	0.1	543.7

**Supplemental Table 5: Active and passive cell properties for colonic supernatant current-clamp experiments (related to Figure 9).**

	<b>PP+SAL</b>	<b>PP+VAN</b>	<b>MP+SAL</b>	<b>MP+VAN</b>
<b>C<sub>Mem</sub> (pF)</b>	13.3±1.9	12.0±1.3	13.7±1.3	13.7±2.0
<b>R<sub>Series</sub> (MΩ)</b>	6.6±0.6	7.4±1.0	6.0±0.6	5.7±0.7
<b>V<sub>Rest</sub> (mV)</b>	-48.2±2.0	-51.3±2.0	-51.9±1.9	-56.5±2.3
+3 μM morphine	-47.8±2.4	-50.0±1.5	-52.0±1.5	-56.0±2.5
<b>AP (2x rheobase)</b>	1.2±0.1	1.1±0.1	2.1±0.3	2.0±0.3
+3 μM morphine	1.1±0.1	1.1±0.1	1.9±0.3	1.1±0.1***
<b>Rheobase (nA)</b>	1.00±0.15	0.77±0.13	0.81±0.11	0.99±0.12
+3 μM morphine	1.20±0.19	0.77±0.13	0.87±0.15	1.04±0.17
<b>AP V<sub>Thresh</sub> (mV)</b>	-10.8±2.4	-9.2±1.6	-20.1±1.3	-21.2±2.1
+3 μM morphine	-6.9±2.9***	-4.5±2.6****	-19.7±1.3	-17.4±2.3***
<b>AP V<sub>Peak</sub> (mV)</b>	40.5±6.9	42.0±6.6	33.2±6.0	37.9±2.4
+3 μM morphine	30.8±9.9	40.6±7.5	34.4±6.3	34.4±2.7
<b>R<sub>input</sub> (MΩ)</b>	203.3±46.5	220.5±31.2	189.1±20.8	140.8±11.0
+3 μM morphine	234.6±96.9	264.4±51.0	216.6±44.7	150.8±16.4

## TRANSPARENT METHODS

**Animals.** Male Swiss Webster mice (Harlan Sprague Dawley, Inc. Frederick, MD, USA) weighing 25–30 g were housed five to a cage in animal care quarters under a 12-hour light/dark cycle with food and water available *ad libitum*. All animal procedures were conducted in accordance with the procedures reviewed and approved by the Institutional Animal Care and Use committee at Virginia Commonwealth University (VCU IACUC).

**Group sizes.** The sample size “N” for each experimental condition is provided in the results and figure legends. These values represent independent observations, not replicates. For patch-clamp experiments, “N” represents the total number of animals, and “n” the total number of cells.

**Randomization.** All animals were randomly divided into control and treatment groups.

**Oral vancomycin treatment.** Vancomycin (Sigma-Aldrich, St. Louis, MO) was administered at 10 mg/kg via oral gavage every 12 hours for 10 days, unless otherwise indicated. Control mice received saline gavage treatments of identical volume and frequency. For treatment duration studies, vancomycin was administered at 10 mg/kg via oral gavage every 12 hours for 5, 10, or 15 days. For all groups, morphine pellets were implanted 5 days prior to the final testing day.

**Chronic morphine treatment.** For chronic morphine administration, a 75 mg morphine or placebo pellet was implanted subcutaneously on the dorsum. Mice were anesthetized with 2.5% isoflurane before shaving the hair from the base of the neck. The skin was cleansed with 10% povidone iodine (General Medical Corp., Walnut, CA) and rinsed with alcohol before making a 1 cm horizontal incision at the base of the neck. The subcutaneous space was opened by insertion of a sterile glass rod toward the dorsal flanks. The pellet was inserted in the space before closing the site with Clay Adams Brand, MikRon AutoClip 9-mm Wound Clips (Becton Dickinson, Franklin Lakes, NJ) and cleansing the surgical site again with 10% povidone iodine. Maintenance of a stringent aseptic surgical field minimized any potential contamination of the pellet, incision, and subcutaneous space. The animals were allowed to recover in their home cages where they remained throughout the experiment.

**Tail-immersion assay.** To test nociceptive responses, the tail-immersion assay was used in this study. Mice were gently detained in a cloth, and the distal 1/3 of the tail immersed in a water bath at 52°C. The latency to tail-flick was recorded, with a maximum latency of 10 sec (to prevent tissue damage). Acute morphine challenge (10 mg/kg, s.c.) was administered 25 min prior to testing.

**DRG isolation.** Dorsal root ganglia were harvested from spinal levels supplying the distal alimentary canal (L<sub>5</sub>-S<sub>1</sub>; modified from Malin et al., 2007) and immediately placed in cold (4 °C) Hanks' balanced salt solution (HBSS; ThermoFisher Scientific, Waltham, MA). Ganglia were incubated (37°C) for 18 min in HBSS with 15 U/mL papain, washed, and incubated for 1 hour in HBSS with 1.5 mg/mL *Clostridium histolyticum* collagenase. Tissues were gently triturated and centrifuged for 5 min at 1,000 rpm. The supernatant was decanted, and cells resuspended in neurobasal A medium containing 1% fetal bovine serum (FBS), 1x B-27 supplement, 10 ng/mL glial cell line-derived neurotrophic factor (GDNF, Neuromics, Edina, MN), 2 mM L-glutamine (ThermoFisher Scientific, Waltham, MA), and penicillin/streptomycin/amphotericin B. The suspension was plated on poly-D-lysine- and laminin-coated coverslips (ThermoFisher Scientific, Waltham, MA) and incubated (37°C) for 24 hr.

**Colonic supernatants.** Full circumference colon segments 5 mm in length were resected from each treatment group and incubated (37°C) for 24 hours in 200 µL of neurobasal A medium containing 1% fetal bovine serum (FBS), 1x B-27 supplement, 10 ng/mL glial cell line-derived neurotrophic factor (GDNF, Neuromics, Edina, MN), 2 mM L-glutamine (ThermoFisher Scientific, Waltham, MA), and penicillin/streptomycin/amphotericin B. The supernatants were then transferred to freshly isolated naïve DRG neuron cultures. An additional 200 µL of fresh medium is added to the cultures before incubating (37°C) for 24 hours. (Protocol adapted from Valdez-Morales et al., 2013 and depicted in *Supplemental Figure 3*.)

**Electrophysiology.** Coverslips were transported to an inverted microscope and continuously superfused with external physiologic saline solution (PSS) at room temperature (20°C). A GΩ seal was achieved via pulled

(Model P-97 Flaming/Brown Micropipette Puller, Sutter Instruments, CA) and fire-polished (2–4 M $\Omega$ ) borosilicate glass capillaries (World Precision Instruments, Sarasota, FL) filled with internal PSS. Standard patch-clamp techniques were performed using an Axopatch 200B amplifier (Molecular Devices, Sunnyvale, CA), Digidata 1440A digitizer, and associated Clampex and Clampfit 10.2 software. All records were performed in whole-cell configuration with digitization at 10 kHz sampling frequency and 5 kHz low-pass Bessel filtering. Only low capacitance (< 30 pF) neurons with healthy morphology and resting membrane potentials more negative than -40 mV were selected for analysis. These cells have been demonstrated to possess characteristics associated with nociceptors, including C and A $\delta$  fiber types, capsaicin sensitivity, long action potential duration, and tetrodotoxin-resistant action potentials (Gold, Shuster and Levine, 1996; Yoshimura and de Groat, 1999; Moore *et al.*, 2002; Beyak *et al.*, 2004; Jin *et al.*, 2013). All recordings were performed 5 min after breakthrough to allow dialysis of internal solution. Cells displaying instability of seal resistance, variable access resistance, or rundown of currents were excluded from the study. No leak subtraction techniques were employed.

For current-clamp experiments, external PSS contained (in mM) 135 NaCl, 5.4 KCl, 0.33 NaH<sub>2</sub>PO<sub>4</sub>, 5 HEPES, 1 MgCl<sub>2</sub>, 2 CaCl<sub>2</sub>, and 5 glucose (pH adjusted to 7.4 with 1 M NaOH). Internal PSS contained (in mM) 100 L-aspartic acid (K salt), 30 KCl, 4.5 Na<sub>2</sub>ATP, 1 MgCl<sub>2</sub>, 10 HEPES, 0.1 EGTA, and 0.5 NaGTP (pH adjusted to 7.2 with 3 M KOH). The observed liquid-junction potential of -12.0 mV was not corrected. Current-clamp step protocols consisting of a 0 nA resting current and 0.03 nA steps from -0.03 nA were employed to assess passive and active cell properties. A short (5 ms) pulse was utilized for assessment of threshold potential and rheobase. A long (100 ms) pulse was utilized to assess the number of action potentials at double rheobase. Taking the derivative of the voltage with respect to time ( $dV/dt$ ), threshold potentials were defined as the voltage at which  $dV/dt$  significantly deviated from zero in the course of an action potential uprise. Records were conducted at 1 min intervals for 10 min. The maximum effect of morphine was recorded for each cell.

For voltage-clamp experiments, external solution supplemented with 1  $\mu$ M TTX contained (in mM) 70 NaCl, 65 NMDG, 5.4 CsCl, 0.33 NaH<sub>2</sub>PO<sub>4</sub>, 5 HEPES, 2.95 MgCl<sub>2</sub>, 0.05 CaCl<sub>2</sub>, and 5 glucose (pH adjusted to 7.4 with concentrated HCl). Internal PSS contained (in mM) 100 CsF, 30 CsCl, 4.5 Na<sub>2</sub>ATP, 1 MgCl<sub>2</sub>, 10 HEPES, 6 EGTA, and 0.5 NaGTP (pH adjusted to 7.2 with 1 M CsOH). The calculated liquid-junction potential of -10.2 mV was not corrected. To assess the voltage-dependence of activation and steady-state inactivation, a double-pulse protocol was employed. A 50 ms variable conditioning pulse was applied in 5 mV steps from -100 to +50 mV. This was followed by a brief (1 ms) interval at -100 mV, then a 50 ms test pulse at 0 mV. Voltage-clamp errors were minimized by 1) selecting cells with <10 M $\Omega$  series resistance, 2) performing 75–85% series resistance compensation, 3) reducing external [Na<sup>+</sup>] to avoid saturation of the amplifier and diminish current-dependent errors of the clamp voltage, and 4) choosing small, spherical neurons with few projections to reduce space clamp errors. When removed, external Na<sup>+</sup> was replaced by the non-permeable organic monovalent cation NMDG. Cells demonstrating instability of or large deviations from the theoretical equilibrium potential of Na<sup>+</sup> (50.6 mV at 20°C) were excluded from the study. The equilibrium potentials observed in I-V curves are notably all near the value predicted by the Nernst equation (when corrected for the liquid-junction potential). K<sup>+</sup> currents were minimized by replacing internal and external K<sup>+</sup> with Cs<sup>+</sup>. TTX-R Na<sup>+</sup> currents were isolated by 1) supplementing external solution with 1  $\mu$ M TTX, 2) replacing internal and external K<sup>+</sup> with Cs<sup>+</sup> (K<sup>+</sup> channel blocker), and 3) eliminating significant influence by Ca<sup>2+</sup> currents by reducing external Ca<sup>2+</sup> and increasing the internal concentration of EGTA (slow Ca<sup>2+</sup> chelator). When removed, external Ca<sup>2+</sup> was replaced by Mg<sup>2+</sup> to preserve surface charge screening.

TTX-R Na<sup>+</sup> current-voltage (I-V) relationships were constructed using peak inward currents elicited at each potential of the conditioning pulse. Where indicated, data are presented as either raw current density (pA/pF) or values normalized to the maximum inward current density between baseline and acute morphine challenge. To map voltage-dependence of activation, observed current densities were transformed to relative conductances ( $G/G_{max}$ ). Observed current densities were taken as a fraction of expected current densities under conditions of maximum conductance by extrapolating the Ohmic portion of the I-V curve. The resulting values were fit with a single Boltzmann function  $G/G_{max} = 1/(1+\exp[(V-V_{1/2}]/k))$ , where  $G/G_{max}$  is relative conductance,  $V$  is command potential,  $V_{1/2}$  is the potential of half-maximum activation, and  $k$  is the slope factor. For steady-state inactivation studies, the relative peak current density ( $I/I_{max}$ ) elicited by the test pulse was plotted as a function of the conditioning pulse potential and fit with a single Boltzmann function. Inactivation time constants ( $\tau_{inactiv}$ ) were then estimated by fitting a monoexponential function to the falling phase of the current traces.

**Statistical analysis.** Statistical differences were calculated as indicated throughout the text using GraphPad Prism 7 (GraphPad Software, Inc., La Jolla, CA). A significance threshold of  $\alpha=0.05$  was utilized for all analyses. Two-group comparisons were performed via two-tailed paired or unpaired Student's t-tests. Multiple-group comparisons were performed via standard or two-way repeated-measures ANOVA with Bonferroni post-hoc analysis. Boltzmann fit models were compared by ordinary least squares non-linear regression, reporting F-ratio test statistics ( $F$ ) and differences in Akaike Information Criterion ( $\Delta AIC$ ) as metrics of differences between model parameters. Results are expressed as mean value  $\pm$  SEM.

## SUPPLEMENTAL REFERENCES

- Beyak, MJ, Ramji, N, Krol, KM, Kawaja, MD, and Vanner, SJ (2004). Two TTX-resistant Na<sup>+</sup> currents in mouse colonic dorsal root ganglia neurons and their role in colitis-induced hyperexcitability. *American Journal of Physiology - Gastrointestinal and Liver Physiology*. 287, G845-G855.
- Gold, MS, Reichling, DB, Shuster, MJ, and Levine, JD (1996). Hyperalgesic agents increase a tetrodotoxin-resistant Na<sup>+</sup> current in nociceptors. *Proceedings of the National Academy of Sciences USA*. 93(3), 1108-1112.
- Jin, X, Shah, S, Liu, Y, Zhang, H, Lees, M, Fu, Z, Lippiat, JD, Beech, DJ, Sivaprasadarao, A, Baldwin, SA, Zhang, H, and Gamper, N (2013). Activation of the Cl<sup>-</sup> channel ANO1 by localized calcium signals in nociceptive sensory neurons requires coupling with the IP3 receptor. *Science Signaling*. 6(290), ra73.
- Malin, SA, Davis, BM, and Molliver, DC (2007). Production of dissociated sensory neuron cultures and considerations for their use in studying neuronal function and plasticity. *Nature Protocols*. 2(1), 152-160.
- Moore, BA, Stewart, TM, Hill, C, and Vanner, SJ (2002). TNBS ileitis evokes hyperexcitability and changes in ionic membrane properties of nociceptive DRG neurons. *American Journal of Physiology - Gastrointestinal and Liver Physiology*. 282, G1045-1051.
- Valdez-Morales, EE, Overington, J, Guerrero-Alba, R, Ochoa-Cortes, F, Ibeakanma, CO, Spreadbury, I, Bunnett, NW, Beyak, M, and Vanner, SJ (2013). Sensitization of peripheral sensory nerves by mediators from colonic biopsies of diarrhea-predominant irritable bowel syndrome patients: A role for PAR2. *The American Journal of Gastroenterology*. 108(10), 1634-1643.
- Yoshimura, N and de Groat, WC (1999). Increased excitability of afferent neurons innervating rat urinary bladder after chronic bladder inflammation. *The Journal of Neuroscience*. 19(11), 4644-4653.